Pet. Sci. (2017) 14:302–314
DOI 10.1007/s12182-017-0155-4

ORIGINAL PAPER

# Carbon isotopic fractionation during vaporization of low molecular weight hydrocarbons ($C_6$–$C_{12}$)

**Qian-Yong Liang[1,2] · Yong-Qiang Xiong[2] · Jing Zhao[1] · Chen-Chen Fang[3] · Yun Li[2]**

Received: 19 August 2016 / Published online: 25 April 2017


**Abstract** Three series of laboratory vaporization experiments were conducted to investigate the carbon isotope fractionation of low molecular weight hydrocarbons (LMWHs) during their progressive vaporization. In addition to the analysis of a synthetic oil mixture, individual compounds were also studied either as pure single phases or mixed with soil. This allowed influences of mixing effects and diffusion though soil on the fractionation to be elucidated. The LMWHs volatilized in two broad behavior patterns that depended on their molecular weight and boiling point. Vaporization significantly enriched the $^{13}C$ present in the remaining components of the $C_6$–$C_9$ fraction, indicating that the vaporization is mainly kinetically controlled; the observed variations could be described with a Rayleigh fractionation model. In contrast, the heavier compounds ($n$-$C_{10}$–$n$-$C_{12}$) showed less mass loss and almost no significant isotopic fractionation during vaporization, indicating that the isotope characteristics remained sufficiently constant for these hydrocarbons to be used to identify the source of an oil sample, e.g., the specific oil field or the origin of a spill. Furthermore, comparative studies suggested that matrix effects should be considered when the carbon isotope ratios of hydrocarbons are applied in the field.

**Keywords** Low molecular weight hydrocarbons · Gas chromatography–isotope ratio mass spectrometry · Isotope fractionation · Vaporization

## 1 Introduction

The $C_6$–$C_{12}$ low molecular weight hydrocarbons (LMWHs) are an important part of petroleum, consisting of different compound classes (*n*-, *iso*-, *cyclo*-alkanes, and aromatics). Various parameters based on the chemical and isotopic compositions of these LMWHs have been widely utilized to make oil/source correlations (Bjorøy et al. 1994; Ten Haven 1996; Odden et al. 1998; Whiticar and Snowdon 1999; Obermajer et al. 2000; Wever 2000), assess the thermal maturity of oils and condensates (Thompson 1983; Mango 2000), determine the source allocation of mixed oils (Chung et al. 1998; Rooney et al. 1998), and identify various secondary alterations of crude oils (George et al. 2002; Pasadakis et al. 2004; Zhang et al. 2005). The characterization of these light compounds is also a powerful tool for tracing the source of petroleum-related contaminants and understanding the environmental processes that control the transport and fate of these contaminants (Dempster et al. 1997; Kelley et al. 1997; Gray et al. 2002; Kolhatkar et al. 2002; Mancini et al. 2002, 2008; Smallwood et al. 2002; Zwank et al. 2003).

Liquid petroleum hydrocarbons, particularly LMWHs, lose mass through vaporization, which can occur in a wide variety of settings, including during the weathering of oil spills (i.e., before sampling), and during sampling, transportation, and storage. The different vaporization behavior

✉ Yong-Qiang Xiong
xiongyq@gig.ac.cn

[1] Key Laboratory of Marine Mineral Resources, Guangzhou Marine Geological Survey, Ministry of Land and Resources, Guangzhou 510760, Guangdong, China

[2] State Key Laboratory of Organic Geochemistry, Guangzhou Institute of Geochemistry, Chinese Academy of Sciences, Guangzhou 510640, Guangdong, China

[3] PetroChina Research Institute of Petroleum Exploration and Development, Beijing 100083, China

Edited by Jie Hao

of each component of an oil sample will alter the sample's chemical and isotopic composition, thus likely influencing the application of some identification methods based on these properties (Cañipa-Morales et al. 2003). It is therefore essential to clarify the possible effects of vaporization on the composition of oil samples prior to the interpretation of the data.

Numerous studies have examined the effects of evaporation on the composition of LMWHs (Thompson 1987, 1988; Cañipa-Morales et al. 2003). Strict collection and preservation procedures are required to avoid the evaporation of a crude oil sample to facilitate the accurate determination of its LMWHs distribution, because even minor evaporation would affect the quality of the data (Cañipa-Morales et al. 2003). Although compound-specific isotope analysis (CSIA) has become a powerful tool for oil characterization and correlation (Chung et al. 1998; Odden et al. 1998; Harris et al. 1999; Whiticar and Snowdon 1999), few studies have considered the effect of evaporation on the $\delta^{13}C$ values of LMWHs (Harrington et al. 1999; Shin and Lee 2010).

In addition, different volatile organic compounds have shown different carbon isotope fractionation trends during evaporation. For example, the enrichment of $^{13}C$ in the vapor fraction was reported for the evaporation of benzene, toluene, ethylbenzene, and xylene (collectively known as BTEX) ($\Delta^{13}C_{vapor-liquid} \approx +0.2‰$) (Harrington et al. 1999), trichloroethylene ($\Delta^{13}C_{vapor-liquid} = +0.1‰$ to $+0.7‰$) (Poulson and Drever 1999), chlorinated aliphatic hydrocarbons ($\Delta^{13}C_{vapor-liquid} = +0.31‰$ for trichloroethene and $\Delta^{13}C_{vapor-liquid} = +0.65‰$ for dichloromethane) (Huang et al. 1999), and MTBE (*tert*-butyl methyl ether, $\Delta^{13}C_{vapor-liquid} = +0.2–0.5‰$ in different physical contexts) (Kuder et al. 2009). The enrichment of $^{13}C$ in the vapor phase could be explained by higher vapor pressure of $^{13}C$-substituted organic compounds relative to $^{12}C$-substituted organic compounds (Baertschi et al. 1953; Narten and Kuhn 1961; Jancso and Van Hook 1974). In contrast, some evaporation experiments have shown that progressive evaporation considerably enriches the remaining liquid fraction in $^{13}C$, with $\Delta^{13}C_{vapor-liquid} = -0.58‰$ and $-0.41‰$ for benzene and toluene, respectively (Shin and Lee 2010). Kinetic fractionation was evidently dominant in controlling the carbon isotopic fractionation during these evaporation experiments.

Previous experimental studies have investigated the evaporation of LMWHs mainly by simulating the evaporation of one or two pure components in each experiment and determining their composition and isotope fractionation at different stages during the evaporation (Huang et al. 1999; Poulson and Drever 1999; Shin and Lee 2010). The effect of the matrix in which the vaporization of a hydrocarbon is studied has seldom been discussed in these experimental studies. However, crude oils and oil products generally comprise a complicated mixture of hydrocarbons, and the matrix effect of the other components may to some extent influence the evaporation behavior of each individual compound.

Additionally, evaporation in natural environments commonly involves other media such as water and soils. A few studies have explored the effects of mixture with water and adsorption to soil on carbon isotope fractionation (Harrington et al. 1999; Slater et al. 1999; Höhener et al. 2003; Schüth et al. 2003; Bouchard et al. 2008a, b). No significant carbon isotope fractionation was observed during the equilibrium vaporization of aqueous solution of toluene and trichloroethylene (Slater et al. 1999), the soil adsorption of BTEX (Harrington et al. 1999) and the sorption of halogenated hydrocarbon compounds (trichloroethene, *cis*-dichloroethene, vinylchloride) and BTEX compounds onto activated carbon, lignite coke, and lignite (Schüth et al. 2003). However, significant fractionation has been observed after passing some volatile organic compounds across alluvial sand (e.g., $\Delta^{13}C_{vapor-liquid}$ is $-2.14 \pm 0.22‰$, $-1.73 \pm 0.52‰$, and $-1.55 \pm 0.45‰$ for *n*-pentane, *n*-hexane, and benzene, respectively) (Bouchard et al. 2008b), and an unsaturated soil zone (Bouchard et al. 2008a). Therefore, the matrix effects (of both mixing and soil diffusion) on the evaporation fractionation should be better understood prior to utilizing the $\delta^{13}C$ value of volatile organic compounds.

The main purpose of this research is to gain better insights into carbon isotope fractionation during the vaporization of $C_6$–$C_{12}$ LMWHs and to determine the influences of multi-component mixtures and soil diffusion on the vaporization of these hydrocarbons. Three series of laboratory vaporization experiments were conducted at room temperature. The first investigated the vaporization of a mixture of $C_6$–$C_{12}$ LMWHs by assessing their vaporization characteristics in a mixture compounds. The second series compared the vaporization of individual pure single-phase compounds. The third series examined vaporization in soil.

## 2 Experimental

### 2.1 Reagents and chemicals

*n*-Hexane (*n*-$C_6$, 99%), *n*-heptane (*n*-$C_7$, HPLC grade, 99+%), *n*-octane (*n*-$C_8$, 98+%), *n*-nonane (*n*-$C_9$, 99%), *n*-decane (*n*-$C_{10}$, 99%), *n*-undecane (*n*-$C_{11}$, 99%), *n*-dodecane (*n*-$C_{12}$, 99+%), benzene (99%), ethylbenzene (99%), *o*-xylene (99%), methylcyclohexane (MCH, 99%), and deuterated *n*-octane (*n*-$C_8D_{18}$, 99%) were purchased from Alfar Aesar China (Tianjin) Co., Ltd. *n*-Pentane (*n*-

$C_5$, 99%) and toluene (99%) were purchased from Qianhui Chemicals and Glassware Co. Ltd. (Guangzhou, China).

The soil used here was first freeze-dried, pulverized with an agate mortar, and then sieved. The fraction with particle sizes less than 100 mesh was heated at 250 °C in an oven for 4 h to eliminate any naturally present LMWHs and microbes. The main minerals in the soil were quartz, chlorite, feldspar, illite, calcite, and dolomite. The total organic carbon of the soil was 0.12%.

### 2.2 Vaporization experiments

Three series of vaporization experiments were designed in which three pure compounds (*n*-hexane, *n*-nonane, and *n*-dodecane) and a mixture of compounds were progressively volatilized in the laboratory. The mixture was of twelve LMWHs, including $C_6$–$C_{12}$ *n*-alkanes, MCH, and BTEX. The mixture was prepared by adding the 12 pure compounds (*n*-$C_6$, 700 μL; benzene, 700 μL; *n*-$C_7$, 400 μL; MCH, 400 μL; toluene, 400 μL; *n*-$C_8$, 300 μL; ethylbenzene, 300 μL; *o*-xylene, 300 μL; *n*-$C_9$, 200 μL; *n*-$C_{10}$, 200 μL; *n*-$C_{11}$, 200 μL; and *n*-$C_{12}$, 200 μL) to a 4-mL glass vial capped with an aluminum–rubber seal.

In the first vaporization experiment, aliquots (approximately 200 μL) of the mixture of compounds were delivered into a series of 4-mL glass vials and weighed. Each vial was then placed in a fume cupboard to allow open vaporization without any agitation, and an air conditioner was used to control the room temperature at 24 ± 1 °C. At intervals up to 72 h, vaporization was measured. For the GC measurement, the vials were then weighed and filled with *n*-pentane. They were tightly capped with aluminum–rubber seals, shaken in an ultrasonicator for 10 min to increase the dissolution of the residue hydrocarbons into the *n*-pentane solvent, and then kept in a freezer prior to analysis.

The second series of vaporization experiments was conducted similar to the first, although instead of the artificial oil mixture, pure compounds were individually studied (*n*-hexane, *n*-nonane, or *n*-dodecane). Aliquots (about 100 μL) of each individual pure compound were added to a series of 4-mL glass vials, and the following procedures for the vaporization experiment were identical to those of the first series.

The third series of vaporization experiments was designed to reveal the effect of diffusion through soil on the vaporization of LMWHs. A certain amount of soil (1 or 2 g) was added to 4-mL glass vials containing a pure hydrocarbon (*n*-hexane or *n*-nonane). Subsequent procedures were as in the preceding series. Finally, the residual compounds were ultrasonically extracted into pentane solvent from the soils.

After vaporization, the concentrations and $\delta^{13}C$ values of the target compounds in the unaltered original sample and the evaporated residual aliquots were measured by directly injecting *n*-pentane solutions containing the target compounds into gas chromatography (GC) and gas chromatography–isotope ratio mass spectrometry (GC–IRMS) apparatus. The remaining fraction ($F$) of each component was calculated by measuring the weight (pure compound) or concentration (artificial oil) of the corresponding compound before and after vaporization.

### 2.3 Gas chromatography (GC)

GC analyses were performed on an Agilent 7890 GC instrument equipped with a split/splitless injector, an HP-PONA fused silica capillary column (50 m × 0.20 mm i.d. × 0.50 μm), and a flame ionization detector. The temperatures for both injection and detection were set at 300 °C. Nitrogen (99.999%) was used as the carrier gas at a maintained constant flow rate of 1.0 mL/min. The injection was operated in split mode (10:1). The GC oven temperature was programmed to rise for 5 min from 35 to 50 °C at a rate of 4 °C/min, and then to 180 °C at 8 °C/min. $C_6$–$C_{12}$ LMWHs were quantified by integration of the peak areas. The response factors of these hydrocarbons relative to the internal standard (*n*-$C_8D_{18}$) were calculated based on the peak area ratios of each $C_6$–$C_{12}$ hydrocarbon compared with the internal standard.

### 2.4 Gas chromatography–isotope ratio mass spectrometry (GC–IRMS)

Carbon isotopic compositions of LMWHs were measured with a gas chromatograph (Agilent 6890) equipped with a DB-5MS column (50 m × 0.25 mm i.d. × 0.25 μm) coupled to an isotope ratio monitoring mass spectrometer (GV IsoPrime). Helium was used as the carrier gas with a maintained constant head pressure of 8.5 psi. The GC oven temperature was programmed to be initially held at 35 °C for 5 min, then raised to 50 °C at 1.5 °C/min, held for 3 min, increased to 53 °C at 0.5 °C/min, and finally increased to 200 °C at 25 °C/min and held for 2 min. The combustion by-product ($H_2O$) was removed by passing the analyte stream through a selectively permeable membrane (Nafion™) with a dry He counter flow. Carbon isotope ratios were computed by five pulses of $CO_2$ reference gas with known $\delta^{13}C$ values (−22.5‰, VPDB), which were injected via the interface to the IRMS instrument at the beginning and end of each analysis. A standard mixture of *n*-alkanes ($C_{12}$–$C_{32}$) from Indiana University with known isotopic composition was used daily to monitor the performance of the instrument. The reported isotopic data represent the arithmetic means of at least two replicate

analyses, and the repeatability is better than ±0.3‰ (VPDB).

### 2.5 Quantification of isotope fractionation during vaporization and diffusion across soil

The experimental isotope factors can be determined using the following Rayleigh equations:

$$R = R_o \cdot F^{\alpha-1} \quad (1)$$

$$\ln A = (\alpha-1) \cdot \ln F \quad (2)$$

$$A = \left(\delta^{13}C_R + 1000\right)/\left(\delta^{13}C_I + 1000\right) \quad (3)$$

where $F$ is the mass fraction of the original compound remaining, $R$ and $R_o$ are the $^{13}C/^{12}C$ value of the individual compound at a specific $F$ ($F < 1$) and at $F = 1$, respectively, and $\alpha$ (equal to $R_{vapor}/R_{liquid}$) is the vapor–liquid fractionation factor. $\delta^{13}C_R$ and $\delta^{13}C_I$ are the $\delta^{13}C$ values of the residual and initial compound, respectively. For each compound of the artificial oil, the $\alpha$ values were calculated by linear regression of $\ln F$ versus $\ln A$.

The corresponding isotope enrichment factors can be calculated according to:

$$\varepsilon(‰) = (\alpha-1) \cdot 1000 \quad (4)$$

The uncertainty was characterized using the standard uncertainty of the slope obtained by linear regression using the least-squares method, which was performed by the data analysis tool installed in Microsoft Excel.

The theoretical fractionation factor between the diffusion coefficients is given by the following equation (Craig 1953; Cerling et al. 1991; Bouchard et al. 2008c; Jeannottat and Hunkeler 2012):

$$\alpha_t = \frac{D_h}{D_l} = \sqrt{\frac{(MW_h + MW_a) \cdot MW_l}{(MW_l + MW_a) \cdot MW_h}} \quad (5)$$

where $D$ represents the diffusion coefficient, MW the molecular weight, and the subscripts l, h, and a represent light isotopes only, molecules with one heavy isotope, and air, respectively ($MW_a = 28.8$ g/mol in this case).

## 3 Results and discussion

An evaporation system with constant boundary conditions will usually have a constant evaporation rate for a single liquid (one component) with respect to time (Stiver and Mackay 1984). In contrast to the linear evaporation of a pure compound, the evaporative loss of a mixture by total weight or volume is either logarithmic (approximately seven or more components) or a square root function (between about five and seven components) with time (Fingas 1997). This implies that the evaporation behavior of a given component is probably different between its pure state (single-component liquid) and when it is in a mixture due to the occurrence of intermolecular interactions. Therefore, the carbon isotope fractionations of LMWHs during evaporation from a mixture and from soil were investigated to explore their evaporation behavior under conditions resembling practical situations.

### 3.1 Carbon isotope fractionations of LMWHs during the progressive vaporization of artificial oil

To eliminate the possible influence of co-elution and other factors on the measurement of the LMWHs, a mixture consisting of twelve pure standards ($n$-$C_6$, benzene, $n$-$C_7$, MCH, toluene, $n$-$C_8$, ethylbenzene, $o$-xylene, $n$-$C_9$, $n$-$C_{10}$, $n$-$C_{11}$, and $n$-$C_{12}$) was selected here to replace a real oil.

The progression of the remaining mass fractions ($F$) and carbon isotope compositions of the individual $C_6$–$C_{12}$ LMWHs in the volatilized residues of the mixture are summarized in Table 1. The mass losses are being observed against time (h). $n$-$C_6$, benzene, $n$-$C_7$, MCH, toluene, $n$-$C_8$, ethylbenzene, and $o$-xylene in the mixture showed expected mass losses, with the lighter compounds being the most volatile, and these compounds in the residual liquid were enriched in $^{13}C$. However, the heaviest compounds ($n$-decane, $n$-undecane, and $n$-dodecane) after 72 h showed mass losses of 66%, 16%, and 1% and $\delta^{13}C_{R-I}$ values of 0.6, 0.4, and 0.2‰ (within the CSIA error), respectively.

Based on their vaporization rates and variations in $\delta^{13}C$ values, the considered LMWHs fall into two categories: a lighter $C_6$–$C_9$ fraction and a heavier $C_{10}$–$C_{12}$ fraction. The lighter fraction volatilized more quickly and showed considerable carbon isotope fractionation. Plots of $F$ versus vaporization time (Fig. 1a) were used to evaluate the vaporization rates of individual LMWHs: The steeper the curve, the faster the vaporization rate. The plots show that the vaporization rates of the LMWHs were inversely related to their boiling points or carbon number and that the individual components of the lighter fraction rapidly evaporated. The residues of individual LMWHs in the lighter fraction became gradually enriched in $^{13}C$ during vaporization (Table 1; Fig. 2). Their $\delta^{13}C_{R-I}$ values reached up to 0.5‰ (beyond the analytical error of CSIA) once 20%–60% of the compounds were removed, and over 3‰ after the evaporation of about 90% of the component.

The heavier fraction evaporated more slowly (Fig. 1a). After 72-h vaporization, the amounts of $n$-$C_{10}$, $n$-$C_{11}$, and $n$-$C_{12}$ remaining in the mixture compounds sample were 34%, 84%, and 99% of the original, respectively (Table 1; Fig. 2). These compounds showed relatively less isotope

**Table 1** Remaining fraction and the corresponding carbon isotopic composition of individual LMWHs in the residual mixture compounds during progressive vaporization (24 ± 1 °C)

| $T^a$ | $F^b$ | $\delta^{13}C \pm SD$ (‰)[c] | $\delta^{13}C_{R-I}$ (‰)[d] | $T^a$ | $F^b$ | $\delta^{13}C \pm SD$ (‰)[c] | $\delta^{13}C_{R-I}$ (‰)[d] | $T^a$ | $F^b$ | $\delta^{13}C \pm SD$ (‰)[c] | $\delta^{13}C_{R-I}$ (‰)[d] |
|---|---|---|---|---|---|---|---|---|---|---|---|
| *n*-$C_6$ | | | | 12 | 0.19 | −26.9 ± 0.16 | 2.4 | 12 | 0.87 | −49.4 ± 0.07 | 0.0 |
| 0 | 1 | −46.1 ± 0.02 | 0.0 | 15 | 0.06 | −24.4 ± 0.05 | 4.8 | 15 | 0.75 | −49.0 ± 0.12 | 0.4 |
| 1 | 0.81 | −45.6 ± 0.03 | 0.5 | *n*-$C_8$ | | | | 20 | 0.66 | −49.4 ± 0.00 | 0.0 |
| 2 | 0.45 | −44.9 ± 0.21 | 1.2 | 0 | 1 | −45.9 ± 0.15 | 0.0 | 24 | 0.56 | −49.3 ± 0.05 | 0.2 |
| 4 | 0.17 | −44.0 ± 0.08 | 2.1 | 2 | 0.96 | −45.9 ± 0.10 | 0.1 | 33 | 0.33 | −48.4 ± 0.24 | 1.0 |
| 6 | 0.03 | −42.1 ± 0.00 | 4.0 | 4 | 0.92 | −45.8 ± 0.13 | 0.1 | 48 | 0.13 | −47.3 ± 0.28 | 2.2 |
| Ben | | | | 6 | 0.85 | −45.7 ± 0.11 | 0.3 | 64 | 0.04 | −44.5 ± 0.06 | 4.9 |
| 0 | 1 | −24.6 ± 0.17 | 0.0 | 12 | 0.54 | −45.6 ± 0.01 | 0.3 | *n*-$C_{10}$ | | | |
| 1 | 0.89 | −24.1 ± 0.22 | 0.5 | 15 | 0.34 | −44.5 ± 0.25 | 1.4 | 0 | 1 | −35.6 ± 0.10 | 0.0 |
| 2 | 0.55 | −23.6 ± 0.03 | 0.9 | 20 | 0.18 | −44.2 ± 0.00 | 1.7 | 2 | 0.96 | −35.8 ± 0.11 | −0.2 |
| 4 | 0.29 | −22.3 ± 0.03 | 2.3 | 24 | 0.12 | −43.6 ± 0.06 | 2.3 | 6 | 0.97 | −35.4 ± 0.10 | 0.1 |
| 6 | 0.10 | −20.6 ± 0.17 | 4.0 | 33 | 0.02 | −39.4 ± 0.00 | 6.5 | 12 | 0.94 | −35.7 ± 0.00 | −0.1 |
| *n*-$C_7$ | | | | EB | | | | 24 | 0.83 | −35.5 ± 0.10 | 0.0 |
| 0 | 1 | −39.4 ± 0.12 | 0.0 | 0 | 1 | −28.3 ± 0.18 | 0.0 | 33 | 0.76 | −35.3 ± 0.05 | 0.3 |
| 1 | 0.97 | −39.3 ± 0.10 | 0.1 | 2 | 0.98 | −28.3 ± 0.09 | 0.0 | 48 | 0.57 | −35.0 ± 0.00 | 0.6 |
| 2 | 0.82 | −39.3 ± 0.07 | 0.2 | 4 | 0.95 | −28.3 ± 0.05 | 0.0 | 64 | 0.40 | −35.0 ± 0.03 | 0.6 |
| 4 | 0.66 | −39.0 ± 0.04 | 0.5 | 6 | 0.90 | −28.1 ± 0.03 | 0.2 | 72 | 0.34 | −34.9 ± 0.05 | 0.6 |
| 6 | 0.46 | −38.2 ± 0.07 | 1.2 | 12 | 0.61 | −28.1 ± 0.06 | 0.2 | *n*-$C_{11}$ | | | |
| 9 | 0.21 | −37.4 ± 0.24 | 2.0 | 15 | 0.41 | −27.0 ± 0.25 | 1.3 | 0 | 1 | −27.8 ± 0.28 | 0.0 |
| 12 | 0.10 | −36.6 ± 0.04 | 2.8 | 20 | 0.22 | −27.2 ± 0.05 | 1.1 | 2 | 0.97 | −27.6 ± 0.07 | 0.2 |
| 15 | 0.02 | −33.5 ± 0.13 | 5.9 | 24 | 0.16 | −26.0 ± 0.05 | 2.3 | 6 | 0.96 | −27.6 ± 0.04 | 0.2 |
| MCH | | | | 33 | 0.03 | −25.1 ± 0.15 | 3.2 | 12 | 0.97 | −27.7 ± 0.03 | 0.2 |
| 0 | 1 | −29.3 ± 0.07 | 0.0 | o-Xy | | | | 24 | 0.97 | −27.5 ± 0.03 | 0.3 |
| 1 | 0.97 | −29.2 ± 0.07 | 0.0 | 0 | 1 | −28.0 ± 0.13 | 0.0 | 33 | 0.94 | −27.7 ± 0.00 | 0.2 |
| 2 | 0.81 | −29.2 ± 0.03 | 0.0 | 2 | 0.99 | −28.1 ± 0.08 | 0.0 | 48 | 0.89 | −27.6 ± 0.00 | 0.3 |
| 4 | 0.66 | −29.0 ± 0.09 | 0.3 | 4 | 0.97 | −28.0 ± 0.16 | 0.0 | 64 | 0.86 | −27.5 ± 0.01 | 0.3 |
| 6 | 0.45 | −28.6 ± 0.07 | 0.7 | 6 | 0.94 | −28.1 ± 0.00 | −0.1 | 72 | 0.84 | −27.5 ± 0.03 | 0.4 |
| 9 | 0.19 | −27.9 ± 0.01 | 1.4 | 12 | 0.72 | −28.0 ± 0.08 | 0.0 | *n*-$C_{12}$ | | | |
| 12 | 0.10 | −27.3 ± 0.07 | 2.0 | 15 | 0.55 | −27.5 ± 0.21 | 0.6 | 0 | 1 | −31.9 ± 0.07 | 0.0 |
| 15 | 0.02 | −25.6 ± 0.05 | 3.7 | 20 | 0.37 | −27.4 ± 0.03 | 0.6 | 2 | 0.98 | −31.9 ± 0.05 | 0.0 |
| Tol | | | | 24 | 0.29 | −27.0 ± 0.03 | 1.1 | 6 | 0.96 | −31.7 ± 0.01 | 0.1 |
| 0 | 1 | −29.3 ± 0.25 | 0.0 | 33 | 0.08 | −24.9 ± 0.00 | 3.1 | 12 | 0.97 | −31.8 ± 0.03 | 0.0 |
| 1 | 0.99 | −29.1 ± 0.23 | 0.1 | *n*-$C_9$ | | | | 24 | 0.99 | −31.7 ± 0.03 | 0.1 |
| 2 | 0.88 | −28.9 ± 0.09 | 0.3 | 0 | 1 | −49.4 ± 0.04 | 0 | 33 | 1.00 | −31.8 ± 0.00 | 0.0 |
| 4 | 0.77 | −28.8 ± 0.12 | 0.5 | 2 | 1.00 | −49.5 ± 0.19 | −0.1 | 48 | 0.97 | −31.9 ± 0.00 | 0.0 |
| 6 | 0.59 | −28.2 ± 0.14 | 1.1 | 4 | 0.98 | −49.3 ± 0.21 | 0.1 | 64 | 0.99 | −31.7 ± 0.03 | 0.2 |
| 9 | 0.36 | −27.4 ± 0.18 | 1.8 | 6 | 0.94 | −49.3 ± 0.06 | 0.2 | 72 | 0.99 | −31.7 ± 0.03 | 0.2 |

[a] *t*, time of vaporization (h)

[b] *F*, fraction of original compound remaining

[c] $\delta^{13}C \pm SD$, average ± standard deviation of carbon isotopic composition obtained by three parallel measurements

[d] $\delta^{13}C_{R-I}$, carbon isotope difference between the residual and initial composition

fractionations over the entire process of vaporization, particularly *n*-$C_{11}$ and *n*-$C_{12}$, which showed variations of $\delta^{13}C$ of less than 0.6‰ (Table 1). A similar result was reported in a previous study (Wang and Huang 2003): the $\delta^{13}C$ values of residual $C_{10}$, $C_{11}$, $C_{12}$, $C_{13}$, and $C_{14}$ *n*-alkanes changed by less than ±0.3‰ when 45%, 29%,

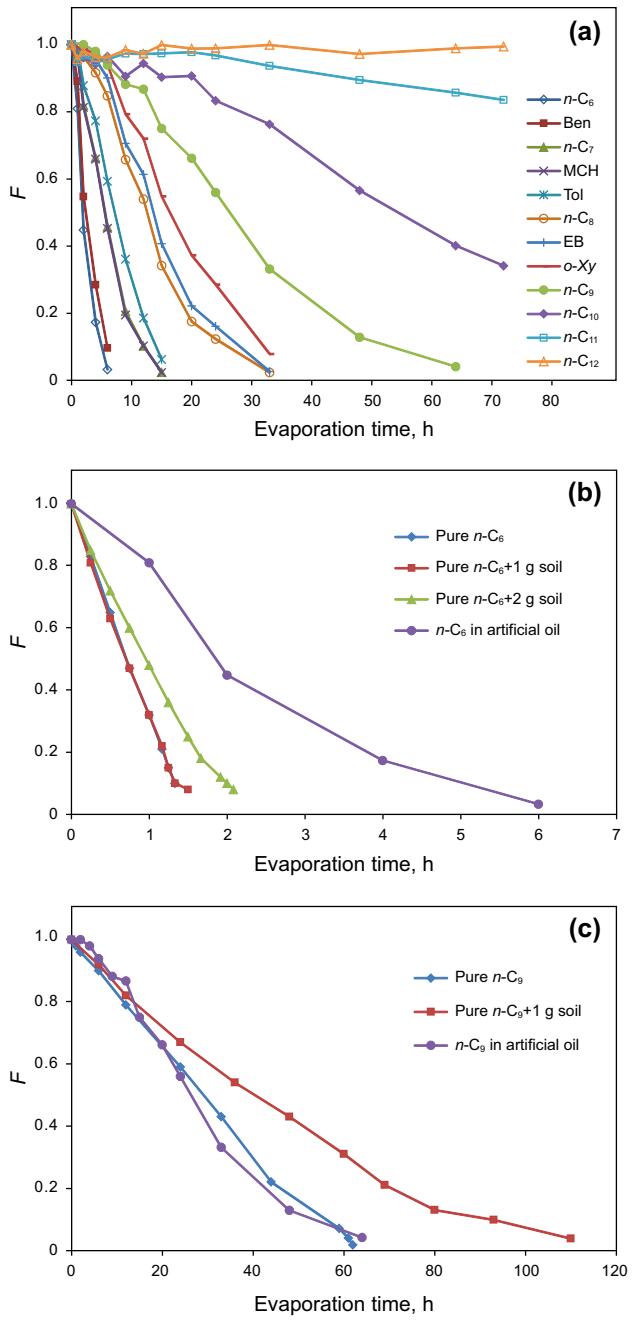


**Fig. 1** Variation of the remaining mass fraction ($F$) as a function of vaporization time. **a** The artificial oil; **b** $n$-hexane; **c** $n$-nonane

30%, 37%, and 51% of the starting compounds remained in the vial, respectively. Therefore, the $\delta^{13}C$ values of the heavier $n$-alkanes varied little enough to make them useful identifiers of oil that has been evaporated to some extent.

Figure 3 shows the good linear correlation between $\ln[(\delta^{13}C_R + 1000)/(\delta^{13}C_I + 1000)]$ and $\ln F$ for the compounds of the lighter fraction, whose regression coefficients ($R^2$) were 0.98 ($n$-$C_6$), 0.99 ($n$-$C_7$), 0.97 ($n$-$C_8$), 0.91 ($n$-$C_9$), 0.996 (MCH), 0.97 (benzene), 0.97 (toluene), 0.91 (ethylbenzene), and 0.93 ($o$-xylene). These results suggest that the carbon isotope fractionations of these compounds during vaporization from a multi-component system (the artificial oil) followed the Rayleigh fractionation model.

**Fig. 2** Carbon isotope fractionation of individual LMWHs in the residual artificial oil ($\delta^{13}C_{R-I}$) versus remaining fraction ($F$) of the corresponding components during progressive vaporization ▶

The vapor–liquid carbon isotope enrichment factor ($\varepsilon$), also sometimes noted by $\Delta^{13}C_{vapor-liquid}$, is considered the best way to express the isotope fractionation effect (Hayes, 1993). All the $\varepsilon$ values observed here were negative, ranging from −0.87 to −1.74‰ ($\varepsilon$ = slope × 1000, Fig. 3), indicating that the progressive vaporization of these compounds was dominated by kinetic fractionation, i.e., the preferential removal of molecules containing the lighter isotope. The same trend was observed by Shin and Lee (2010), who reported enrichment factors for benzene and toluene of −0.58 and −0.41‰, respectively. The magnitude of carbon isotope fractionation during the vaporization of a pure liquid phase appears to be considerably less than that from a multi-component system.

### 3.2 Carbon isotope fractionations of LMWHs during the progressive vaporization of single pure liquid and diffusion through soil

To understand better matrix effects on the carbon isotope fractionation of individual LMWHs during vaporization from a mixture, vaporization experiments of three pure compounds ($n$-hexane, $n$-nonane, and $n$-dodecane) were conducted under the same conditions as the assessment of the artificial oil. Only 7.4% mass loss and no obvious $\delta^{13}C$ variation (<0.5‰, VPDB) were observed for $n$-dodecane after 72 h of vaporization. Consequently, only $n$-hexane and $n$-nonane are discussed.

Table 2 lists the progressive vaporization results for $n$-hexane, both its pure single phase and when in 1 g soil and 2 g soil. The pure single phase lost mass approximately as quickly as when it was mixed with 1 g soil: Both showed mass losses of about 90% after 80 min, with the $\delta^{13}C$ of the residue shifted more than 2.0‰ in both cases. $n$-Hexane in 2 g soil lost about 90% of its mass after 120 min of vaporization, and the $\delta^{13}C$ of the residue shifted 3.3‰. Its maximal $\delta^{13}C$ shift was 3.5‰ after 125 min with a corresponding mass loss of 92%, which represents a much slower mass loss than observed for the pure liquid and the $n$-hexane in 1 g soil. Increasing the mass of soil slowed the vaporization rate and lessened the change of $\delta^{13}C$ of the residue.

Figure 1b shows that $n$-$C_6$ added to 1 g soil volatilized at a similar rate to the pure liquid phase, indicating that

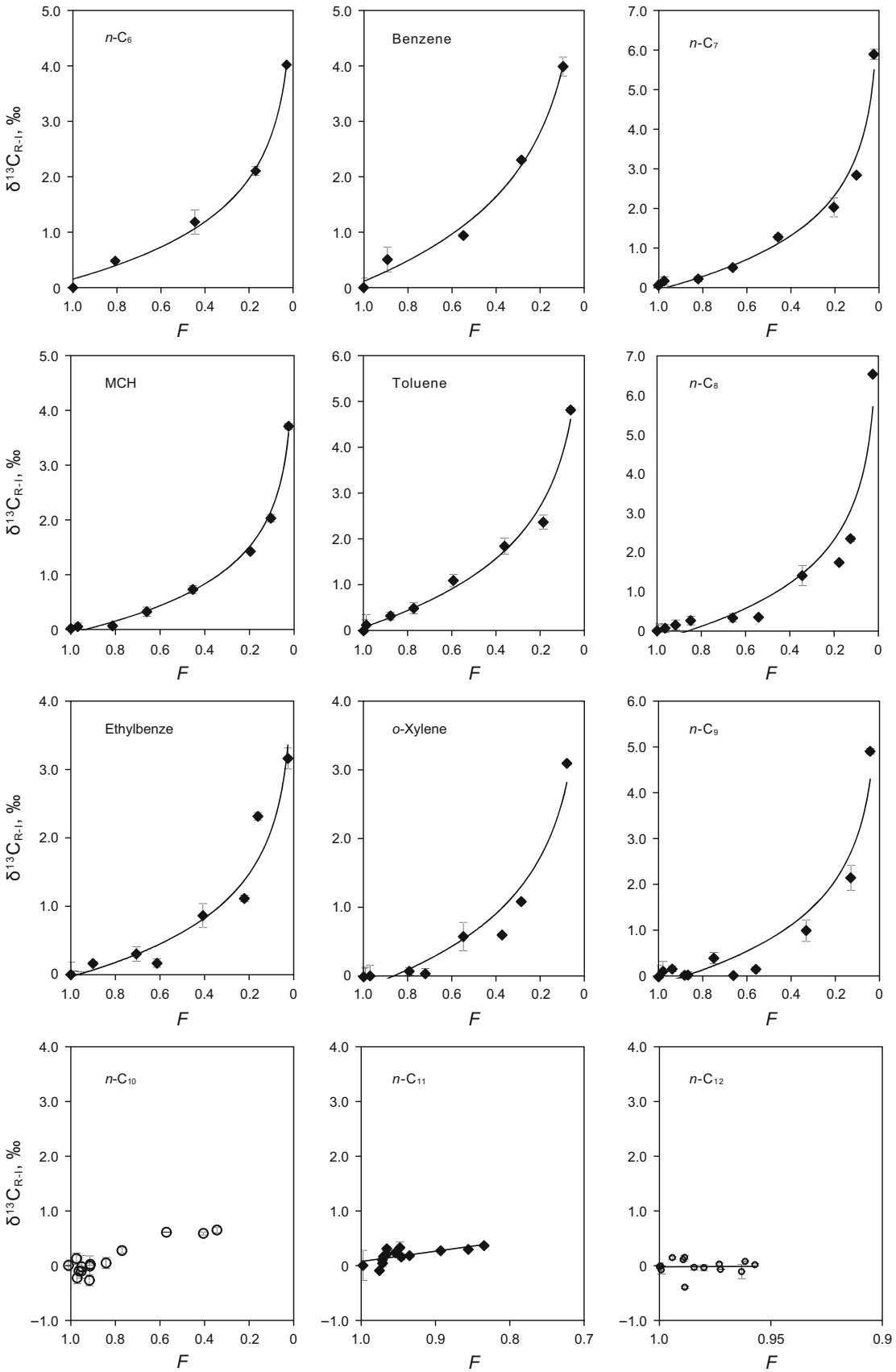
n-C6
Benzene
n-C7
MCH
Toluene
n-C8
Ethylbenze
o-Xylene
n-C9
n-C10
n-C11
n-C12
δ13CR-I, ‰
F

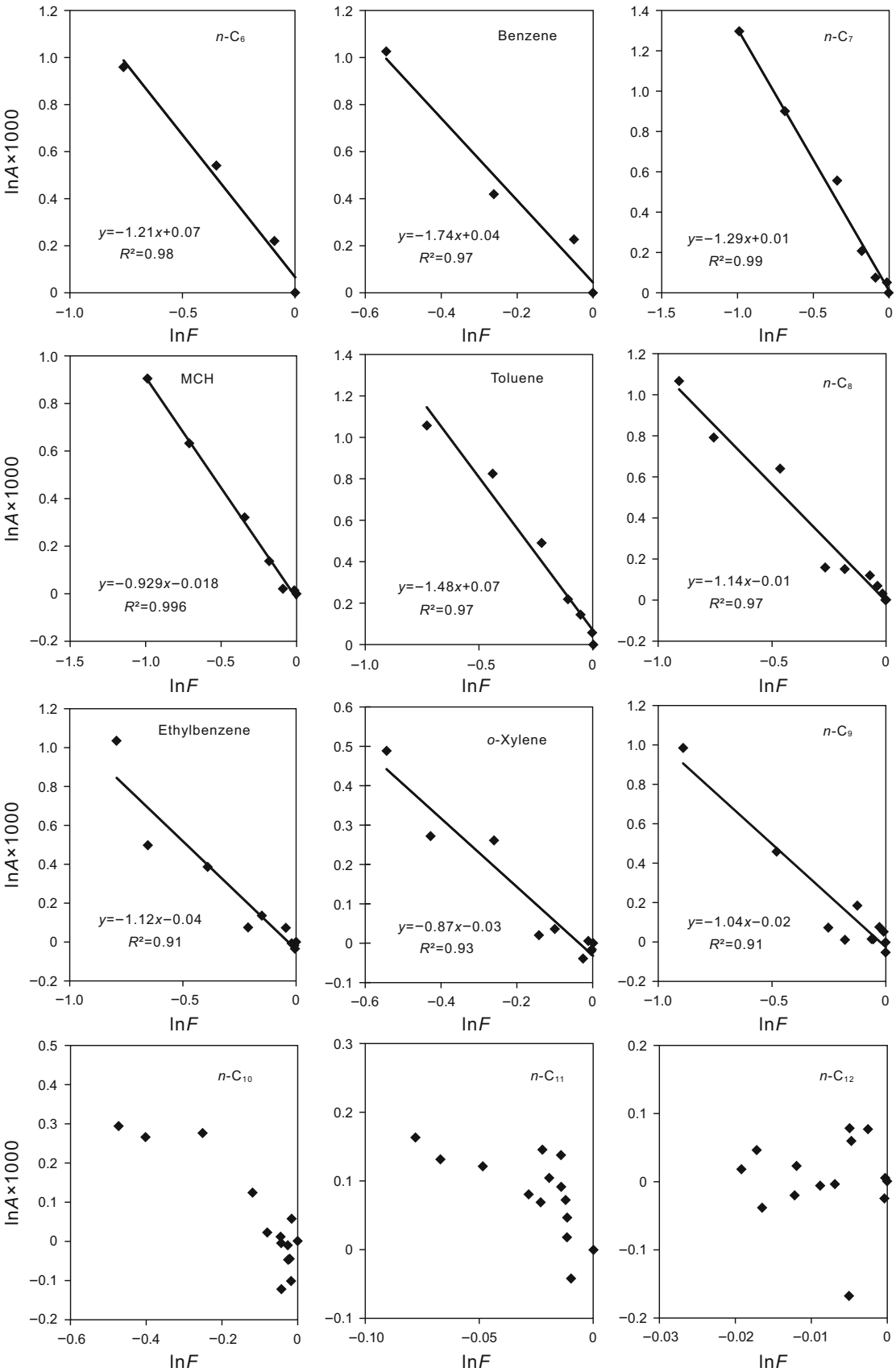
n-C6
y=−1.21x+0.07
R²=0.98
Benzene
y=−1.74x+0.04
R²=0.97
n-C7
y=−1.29x+0.01
R²=0.99
MCH
y=−0.929x−0.018
R²=0.996
Toluene
y=−1.48x+0.07
R²=0.97
n-C8
y=−1.14x−0.01
R²=0.97
Ethylbenzene
y=−1.12x−0.04
R²=0.91
o-Xylene
y=−0.87x−0.03
R²=0.93
n-C9
y=−1.04x−0.02
R²=0.91
n-C10
n-C11
n-C12
lnA×1000
lnF

◀**Fig. 3** Carbon isotope fractionation of individual compounds, as ln$A$, versus fraction of residual liquid, presented as ln$F$, during the progressive vaporization of artificial oil

diffusion through the 1 g soil did not have a remarkable effect on the vaporization of the $n$-$C_6$ owing to its relatively high volatility. Both $n$-$C_9$ in 1 g soil and $n$-$C_6$ in 2 g soil evaporated less quickly than their respective pure compounds. The results show that a LMWH's diffusion through soil can slow its rate of vaporization, with the effect depending on the volatility of the compound.

Table 3 lists the progressive vaporization results of $n$-nonane, both its pure single phase and in 1 g soil. The compound evaporated more slowly in the soil than alone, but it showed a greater $\delta^{13}C$ shift in the soil (Fig. 1c).

The strong correlations between ln$A$ and ln$F$ for $n$-$C_6$ ($R^2 = 0.998$, 0.99, and 0.98 for the pure single phase, in 1 g soil, and in 2 g soil, respectively) and $n$-$C_9$ ($R^2 = 0.99$

**Table 2** Carbon isotopic composition of residual $n$-hexane evaporated as a free phase and from soil (24 ± 1 °C)

| Pure $n$-$C_6$ | | | | Pure $n$-$C_6$ + 1 g soil | | | | Pure $n$-$C_6$ + 2 g soil | | | |
|---|---|---|---|---|---|---|---|---|---|---|---|
| $t$[a] | $F$[b] | $\delta^{13}C \pm SD$ (VPDB, ‰)[c] | $\delta^{13}C_{R-I}$ (‰)[d] | $t$[a] | $F$[b] | $\delta^{13}C \pm SD$ (VPDB, ‰)[c] | $\delta^{13}C_{R-I}$ (‰)[d] | $t$[a] | $F$[b] | $\delta^{13}C \pm SD$ (VPDB, ‰)[c] | $\delta^{13}C_{R-I}$ (‰)[d] |
| 0 | 1 | −46.2 ± 0.08 | 0 | 0 | 1 | −46.2 ± 0.05 | 0 | 0 | 1 | −46.1 ± 0.10 | 0 |
| 15 | 0.83 | −46.0 ± 0.04 | 0.2 | 15 | 0.81 | −45.9 ± 0.12 | 0.2 | 15 | 0.85 | −45.9 ± 0.03 | 0.2 |
| 30 | 0.65 | −45.8 ± 0.08 | 0.5 | 30 | 0.63 | −45.8 ± 0.07 | 0.3 | 30 | 0.72 | −43.9 ± 0.01 | 0.3 |
| 45 | 0.47 | −45.6 ± 0.05 | 0.7 | 45 | 0.47 | −45.6 ± 0.04 | 0.6 | 45 | 0.60 | −45.6 ± 0.04 | 0.5 |
| 60 | 0.32 | −45.1 ± 0.05 | 1.1 | 60 | 0.32 | −45.3 ± 0.11 | 0.9 | 60 | 0.48 | −45.5 ± 0.06 | 0.6 |
| 70 | 0.21 | −44.8 ± 0.09 | 1.4 | 70 | 0.22 | −45.0 ± 0.02 | 1.2 | 75 | 0.36 | −45.1 ± 0.05 | 1.1 |
| 75 | 0.15 | −44.5 ± 0.12 | 1.8 | 75 | 0.15 | −44.5 ± 0.06 | 1.7 | 90 | 0.25 | −44.6 ± 0.05 | 1.6 |
| 80 | 0.10 | −44.1 ± 0.08 | 2.1 | 80 | 0.10 | −44.2 ± 0.11 | 2.0 | 100 | 0.18 | −44.1 ± 0.01 | 2.1 |
| | | | | 85 | 0.08 | −44.0 ± 0.05 | 2.2 | 115 | 0.12 | −43.2 ± 0.08 | 2.9 |
| | | | | | | | | 120 | 0.10 | −42.8 ± 0.09 | 3.3 |
| | | | | | | | | 125 | 0.08 | −42.7 ± 0.07 | 3.5 |

[a] $t$, time of vaporization (min)

[b] $F$, fraction of original compound remaining

[c] $\delta^{13}C \pm SD$, average ± standard deviation of carbon isotopic composition obtained by three parallel measurements

[d] $\delta^{13}C_{R-I}$, carbon isotope difference between the residual and initial composition

**Table 3** Carbon isotopic composition of residual $n$-nonane evaporated as a free phase and from soil

| Pure $n$-$C_9$ | | | | Pure $n$-$C_9$ + 1 g soil | | | |
|---|---|---|---|---|---|---|---|
| $t$[a] | $F$[b] | $\delta^{13}C \pm SD$ (VPDB, ‰)[c] | $\delta^{13}C_{R-I}$ (‰)[d] | $t$[a] | $F$[b] | $\delta^{13}C \pm SD$ (VPDB, ‰)[c] | $\delta^{13}C_{R-I}$ (‰)[d] |
| 0 | 1 | −49.4 ± 0.08 | 0 | 0 | 1 | −49.6 ± 0.06 | 0 |
| 1 | 0.98 | −49.5 ± 0.04 | −0.1 | 6 | 0.92 | −49.5 ± 0.04 | 0.1 |
| 2 | 0.96 | −49.4 ± 0.05 | 0.0 | 12 | 0.82 | −49.4 ± 0.09 | 0.2 |
| 6 | 0.9 | −49.5 ± 0.11 | 0.0 | 24 | 0.67 | −49.3 ± 0.05 | 0.2 |
| 12 | 0.79 | −49.4 ± 0.06 | 0.1 | 36 | 0.54 | −49.2 ± 0.06 | 0.4 |
| 24 | 0.59 | −49.1 ± 0.06 | 0.3 | 48 | 0.43 | −49.0 ± 0.09 | 0.5 |
| 33 | 0.43 | −48.8 ± 0.04 | 0.6 | 60 | 0.31 | −48.7 ± 0.05 | 0.9 |
| 44 | 0.22 | −48.6 ± 0.04 | 0.9 | 69 | 0.21 | −48.5 ± 0.02 | 1.0 |
| 59 | 0.07 | −48.0 ± 0.08 | 1.4 | 80 | 0.13 | −48.1 ± 0.09 | 1.5 |
| 61 | 0.039 | −47.6 ± 0.03 | 1.8 | 93 | 0.098 | −49.6 ± 0.15 | 1.8 |
| 62 | 0.017 | −47.1 ± 0.03 | 2.3 | 110 | 0.038 | −47.2 ± 0.19 | 2.4 |

[a] $t$, time of vaporization (h)

[b] $F$, fraction of original compound remaining

[c] $\delta^{13}C \pm SD$, average ± standard deviation of carbon isotopic composition obtained by three parallel measurements

[d] $\delta^{13}C_{R-I}$, carbon isotope difference between the residual and initial composition

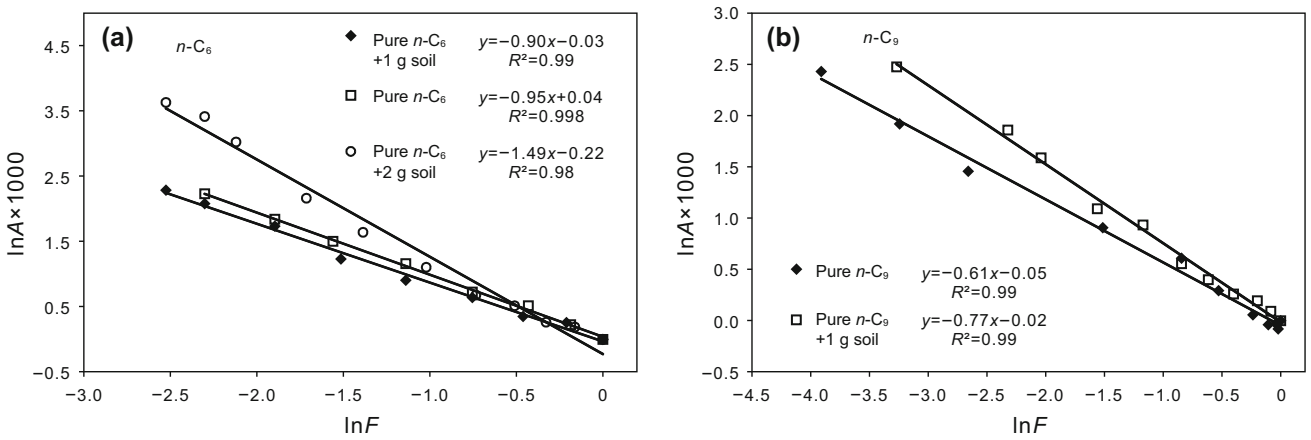


**Fig. 4** Carbon isotope fractionation of vaporization for individual $n$-$C_6$ (**a**) and $n$-$C_9$ (**b**), as ln$A$, versus fraction of residual liquid, presented as ln$F$, during progressive vaporization

and 0.99 for the pure single and in 1 g soil, respectively) (Fig. 4) indicate that the vaporization in each case followed the Rayleigh trend.

### 3.3 Possible mechanism of carbon isotope fractionation of LMWHs during vaporization

Theoretically, the effects of equilibrium vapor pressure (evaporation-controlled) and kinetics (diffusion-controlled) are the two main factors that influence the fractionation of stable isotopes of organic compounds during vaporization, and the competition between them directly determine the direction of the fractionation. The evaporation-controlled process usually results in "inverse isotope fractionation," characterizing of enriching $^{13}C$ in the vapor phase (Baertschi et al. 1953; Balabane and Letolle 1985; Huang et al. 1999; Poulson and Drever 1999; Wang and Huang 2001; Jeannottat and Hunkeler 2012; Xiao et al. 2012), whereas diffusion-controlled vaporization, which depends on the system itself and intermolecular free energy due to the van der Waals attractive forces among molecules, results in the "normal isotope fractionation," characterizing of enriching $^{13}C$ in the residual liquids (Shin and Lee 2010; Xiao et al. 2012; Kuder et al. 2009; Bouchard et al. 2008a, b, c; Jeannottat and Hunkeler 2012; Hayes 1993; Wang and Huang 2001).

Table 4 lists the carbon isotope enrichment factors of the LMWHs considered here and in previous studies, along with values calculated using Eq. (5) (Craig 1953; Cerling et al. 1991; Bouchard et al. 2008c; Jeannottat and Hunkeler 2012). All the experimental values of $\varepsilon$ ($\varepsilon_e$) for the $C_6$–$C_9$ LMWHs are negative, indicating the enrichment of $^{13}C$ in the residual liquids and "normal isotope fractionation" during vaporization. The vaporization of these compounds is thus diffusion-controlled, and the equilibrium vapor pressure has little effect on their natural vaporization.

The $n$-alkanes in the mixture compounds showed decreasing experimental values of $\varepsilon$ with their increasing carbon number (Table 4): Values of $-1.21 \pm 0.06$, $-1.29 \pm 0.14$, $-1.14 \pm 0.23$, and $-1.04 \pm 0.17$‰ were observed with 95% confidence limits for $n$-$C_6$, $n$-$C_7$, $n$-$C_8$, and $n$-$C_9$, respectively. Benzene, toluene, ethylbenzene, and $o$-xylene, respectively, showed values of $-1.74 \pm 0.08$, $-1.48 \pm 0.10$, $-1.12 \pm 0.12$, and $-0.87 \pm 0.09$‰ with 95% confidence limits. These results confirm that the isotope enrichment factor of a compound is controlled by its molecular weight and boiling point. Therefore, the intermolecular binding energies (van der Waals attraction forces) are the main factor controlling the isotope fractionation during the vaporization of the mixture compounds and the single compounds ($n$-$C_6$ and $n$-$C_9$) both as a pure single phase and when in soil.

In a diffusion-limited vaporization system, it is well known that the higher the vapor saturation is above that of volatilizing water, the lower the isotope effects (Craig and Gordon 1965). The results of this study combined with previous results indicate that this rule holds for the vaporization of LMWHs. The carbon isotope enrichment factor of volatilizing pure single-phase $n$-hexane was $-0.95 \pm 0.04$‰ (95% confidence limit, Table 4). While that for pure $n$-hexane volatilizing across 1 g soil, 2 g soil, and a soil column became gradually higher with the progression along the series of matrices in which the vapor space become increasingly unsaturated and the vapor pressures gradually decreased. A similar trend was observed during the vaporization of $n$-$C_9$. This demonstrates the effects of the matrix: diffusion materials like soil can decrease the vapor saturation and make the remaining liquid enriched in $^{13}C$, further increasing the isotope enrichment factor.

$n$-$C_{10}$, $n$-$C_{11}$, and $n$-$C_{12}$, on the other hand, showed little change in isotopic composition with mass loss (or lack

**Table 4** Comparison of experimental carbon isotope enrichment factors of this work, previous studies, and the theoretical enrichment factors of LMWHs during vaporization

| Compound | $\varepsilon_e^a$ (‰) | 95% CI[b] | Experimental material | $\alpha_t^c$ | $\varepsilon_t^d$ (‰) | References |
|---|---|---|---|---|---|---|
| *n*-$C_6$ | −1.21 | ±0.06 | Artificial oil | 0.99856 | −1.44 | This study |
| | −0.95 | ±0.04 | Pure liquid | | | |
| | −0.90 | ±0.07 | In 1 g soil | | | |
| | −1.49 | ±0.18 | In 2 g soil | | | |
| | −1.73 | ±0.52 | Soil column | | | Bouchard et al. (2008b) |
| | −1.02 | / | Natural oil | | | Xiao et al. (2012) |
| *n*-$C_7$ | −1.29 | ±0.14 | Artificial oil | 0.99889 | −1.11 | This study |
| | −1.01 | / | Natural oil | | | Xiao et al. (2012) |
| *n*-$C_8$ | −1.14 | ±0.23 | Artificial oil | 0.99912 | −0.88 | This study |
| | −0.57 | / | Natural oil | | | Xiao et al. (2012) |
| *n*-$C_9$ | −1.04 | ±0.17 | Artificial oil | 0.99929 | −0.71 | This study |
| | −0.61 | ±0.08 | Pure liquid | | | |
| | −0.77 | ± 0.06 | In 1 g soil | | | |
| Benzene | −1.74 | ±0.08 | Artificial oil | 0.99829 | −1.71 | This study |
| | −1.55 | ±0.45 | Soil column | | | Bouchard et al. (2008b) |
| | −0.58 | ±0.04 | Pure liquid | | | Shin and Lee (2010) |
| MCH | −0.93 | ±0.04 | Artificial oil | 0.99885 | −1.15 | This study |
| | −0.60 | / | Natural oil | | | Xiao et al. (2012) |
| Toluene | −1.48 | ±0.10 | Artificial oil | 0.99872 | −1.28 | This study |
| | −0.41 | ±0.04 | pure liquid | | | Shin and Lee (2010) |
| | −1.48 | / | Natural oil | | | Xiao et al. (2012) |
| Ethylbenzene | −1.12 | ±0.12 | Artificial oil | 0.99900 | −1.00 | This study |
| *o*-Xylene | −0.87 | ±0.09 | Artificial oil | 0.99900 | −1.00 | This study |

[a] $\varepsilon_e$, experimental enrichment factors calculated in this work

[b] CI, confidence interval used to elucidate enrichment factors; this was performed by the data analysis tool installed in Microsoft Excel

[c] $\alpha_t$, theoretical fractionation factor calculated by Eq. (5)

[d] $\varepsilon_t$, theoretical enrichment factor

/, not mentioned

thereof) during vaporization. The isotopic composition of the residual liquids varied almost within the CSIA error for these compounds (Table 1; Fig. 1a). This may be because (1) these hydrocarbons are heavier than those in the lighter fraction, and their strong intermolecular binding energies reduced their evaporation rates and (2) the vapors of these hydrocarbons approached close to saturation, thus greatly impeding their vaporization, which resulted in them showing greatly lower mass loss than the lighter fraction.

## 4 Conclusions

The effect of vaporization on the carbon isotopic compositions of LMWHs was investigated through three series of experiments examining a mixture of compounds and pure compounds both alone in a single state and when diffusing across soil. Most of the mixture compounds showed obvious mass loss during vaporization, with the rate of vaporization decreasing with the increasing carbon number of the compounds, indicating that molecular weight and boiling point were the main regulator of that vaporization.

Isotope analysis showed that the vaporization patterns of the $C_6$–$C_{12}$ LMWHs could be classified into two types: one for the lighter $C_6$–$C_9$ fraction and another for the heavier $C_{10}$–$C_{12}$ fraction. The remaining portion of the lighter fraction was significantly enriched in $^{13}C$ by vaporization, with the vaporization fractionation of each hydrocarbon following the Rayleigh model, indicating that kinetic isotope effects controlled the natural vaporization of the molecules and their diffusion through soils. Additionally, significant isotope enrichments (more than 3‰) were apparent in the $\delta^{13}C_{R-I}$ values of the corresponding compounds when more than 90% of each components of the lighter fraction had evaporated. In contrast, the heavier fraction remained isotopically consistent due to its lower mass loss during the vaporization, indicating that the isotopic characteristics of these heavier hydrocarbons could

be extremely useful for identifying the source of a given oil sample, even one slightly evaporated.

Comparison of all the series of studies conducted here suggests that both mixing a given hydrocarbon and its diffusion through soil could slow its vaporization and increase its carbon isotope enrichment factors, because both the mixture and the soil decreased the vapor pressure in the vapor–liquid system. The values of carbon isotope enrichment factors for the LMWHs are quite close to those calculated from theory and reflect a diffusion-controlled vaporization process during the natural vaporization of the LMWHs.

The $C_6$–$C_{12}$ LMWHs are widely used to identify the source of oil samples, to assess the thermal maturity of oils and condensates, to determine the source allocation of mixed oils, to identify various secondary alterations of crude oils, and to trace the source of petroleum-related contaminants. This study shows that there is significant isotope fractionation during the natural vaporization of the lighter fraction of these hydrocarbons, which means that isotope monitoring using the $C_6$–$C_9$ LMWHs should be used carefully. However, as natural vaporization has little influence on the isotopic compositions of the heavier hydrocarbons in a short time (i.e. within 72 h), these molecules can provide reliable carbon isotope data better than $C_6$–$C_9$ LMWHs for use in petroleum and environmental science.

**Acknowledgements** We are grateful to Chen H. S. for the technical assistance. This work is financially supported by the National "863" Project (Grant No. 2012AA0611401) and the program of the Chinese Academy of Sciences (Grant No. KZCX2-YW-JC103). This is contribution number IS-2343 from Guangzhou Institute of Geochemistry, Chinese Academy of Sciences (GIGCAS). We also acknowledge three anonymous reviewers for their helpful comments and suggestions.



## References

Baertschi P, Kuhn W, Kuhn H. Fractionation of isotopes by distillation of some organic substances. Nature. 1953;171:1018–20.

Balabane M, Letolle R. Inverse overall isotope fractionation effect through distillation of some aromatic molecules (anethole, benzene and toluene). Chem Geol. 1985;52:391–6.

Bjorøy M, Hall PB, Moe RP. Stable carbon isotope variation of *n*-alkanes in Central Graben oils. Org Geochem. 1994;22(3–5):355–81.

Bouchard D, Höhener P, Hunkeler D. Carbon isotope fractionation during volatilization of petroleum hydrocarbons and diffusion across a porous medium: a column experiment. Environ Sci Technol. 2008a;42(21):7801–6.

Bouchard D, Hunkeler D, Gaganis P, et al. Carbon isotope fractionation during diffusion and biodegradation of petroleum hydrocarbons in the unsaturated zone: field experiment at Værløse airbase, Denmark, and modeling. Environ Sci Technol. 2008b;42(2):596–601.

Bouchard D, Hunkeler D, Höhener P. Carbon isotope fractionation during aerobic biodegradation of n-alkanes and aromatic compounds in unsaturated sand. Org Geochem. 2008c;39:23–33.

Cañipa-Morales NK, Garlán-Vidal CA, Guzmán-Vega MA, et al. Effect of evaporation on $C_7$ light hydrocarbon parameters. Org Geochem. 2003;34(6):813–26.

Cerling TE, Solomon DK, Quade J, et al. On the isotopic composition of carbon in soil carbon dioxide. Geochim Cosmochim Acta. 1991;55(11):3403–5.

Chung HM, Walters CC, Buck S, et al. Mixed signals of the source and thermal maturity for petroleum, accumulations from light hydrocarbons: an example of the Beryl field. Org Geochem. 1998;29(1–3):381–96.

Craig H. The geochemistry of the stable carbon isotopes. Geochim Cosmochim Acta. 1953;3(2):53–92.

Craig H, Gordon LI. Stable isotopes in oceanographic studies and paleotemperatures. In: Tongiorgi, E, editor. Conference on stable isotopes in oceanographic studies and paleotemperatures. Spoleto, Italy; 1965. p. 9–130.

Dempster HS, Lollar BS, Feenstra S. Tracing organic contaminants in groundwater: a new methodology using compound–specific isotope analysis. Environ Sci Technol. 1997;31:3193–7.

Fingas MF. Studies on the evaporation of crude oil and petroleum products: I. The relationship between evaporation rate and time. J Hazard Mater. 1997;56(3):227–36.

George SC, Boreham CJ, Minifie SA, et al. The effect of minor to moderate biodegradation on $C_5$–$C_9$ hydrocarbons in crude oils. Org Geochem. 2002;33(12):1293–317.

Gray JR, Lacrampe-Couloume G, Gandhi D, et al. Carbon and hydrogen isotopic fractionation during biodegradation of methyl tert–butyl ether. Environ Sci Technol. 2002;36(9):1931–8.

Harris SA, Whiticar MJ, Eek MK. Molecular and isotopic analysis of oils by solid phase microextraction of gasoline range hydrocarbons. Org Geochem. 1999;30:721–37.

Harrington RR, Poulson SR, Drever JI, et al. Carbon isotope systematics of monoaromatic hydrocarbons: vaporization and adsorption experiments. Org Geochem. 1999;30(8A):765–75.

Huang L, Sturchio NC, Abrajano T, et al. Carbon and chlorine isotope fractionation of chlorinated aliphatic hydrocarbons by evaporation. Org Geochem. 1999;30(8A):777–85.

Höhener P, Duwig C, Pasteris G, et al. Biodegradation of petroleum hydrocarbon vapors: laboratory studies on rates and kinetics in unsaturated alluvial sand. J Contam Hydrol. 2003;66(1–2):93–115.

Hayes JM. Factors controlling $^{13}C$ contents of sedimentary organic–compounds: principles and evidence. Mar Geol. 1993;113(1–2):111–25.

Jancso G, Van Hook WA. Condensed phase isotope effects (especially vapor pressure isotope effects). Chem Rev. 1974;74(6):689–750.

Jeannottat S, Hunkeler D. Chlorine and carbon isotopes fractionation during volatilization and diffusive transport of trichloroethene in the unsaturated zone. Environ Sci Technol. 2012;46(6):3169–76.

Kelley CA, Hammer BT, Coffin RB. Concentrations and stable isotope values of BTEX in gasoline-contaminated groundwater. Environ Sci Technol. 1997;31(9):2469–72.

Kolhatkar R, Kuder T, Philp P, et al. Use of compound-specific stable carbon isotope analyses to demonstrate anaerobic biodegradation of MTBE in groundwater at a gasoline release site. Environ Sci Technol. 2002;36(23):5139–46.

Kuder T, Philp P, Allen J. Effects of volatilization on carbon and hydrogen isotope ratios of MTBE. Environ Sci Technol. 2009;43(6):1763–8.

Mancini SA, Lacrampe-Couloume G, Jonker H, et al. Hydrogen isotopic enrichment: an indicator of biodegradation at a petroleum hydrocarbon contaminated field site. Environ Sci Technol. 2002;36(11):2464–70.

Mancini SA, Devine CE, Elsner M, et al. Isotopic evidence suggests different initial reaction mechanisms for anaerobic benzene biodegradation. Environ Sci Technol. 2008;42(22):8290–6.

Mango FD. Light hydrocarbons as oil maturity indicators. Abstr Pap Am Chem Soc. 2000;219:U687–8.

Narten A, Kuhn W. Genaue bestimmung kleiner dampfdruckunterschiede isotoper verbindungen II. Der $^{13}C/^{12}C$–Isotopieeffekt in tetrachlorkohlenstoff und in Benzol. Helv Chim Acta. 1961;44(6):1474–9.

Obermajer M, Osadetz KG, Fowler MG, et al. Light hydrocarbon (gasoline range) parameter refinement of biomarker-based oil–oil correlation studies: an example from Williston Basin. Org Geochem. 2000;31(10):959–76.

Odden W, Patience RL, van Graas GW. Light hydrocarbon (gasoline range) parameter refinement of biomarker-based oil–oil correlation studies: an example from Williston Basin. Org Geochem. 1998;28(12):823–47.

Pasadakis N, Obermajer M, Osadetz KG. Definition and characterization of petroleum compositional families in Williston Basin, North America using principal component analysis. Org Geochem. 2004;35(4):453–68.

Poulson SR, Drever JI. Stable isotope (C, Cl, and H) fractionation during vaporization of trichloroethylene. Environ Sci Technol. 1999;33(20):3689–94.

Rooney MA, Vuletich AK, Griffith CE. Compound-specific isotope analysis as a tool for characterizing mixed oils: an example from the west of Shetlands area. Org Geochem. 1998;29(1–3):241–54.

Schüth C, Taubald H, Bolaño N, et al. Carbon and hydrogen isotope effects during sorption of organic contaninants on carbonaceous materials. J Contam Hydrol. 2003;64:269–81.

Shin WJ, Lee KS. Carbon isotope fractionation of benzene and toluene by progressive evaporation. Rapid Commun Mass Spectrom. 2010;24(11):1636–40.

Slater GF, Dempster HS, Lollar BS, et al. Headspace analysis: a new application for isotopic characterization of dissolved organic contaminants. Environ Sci Technol. 1999;33(1):190–4.

Smallwood BJ, Philp RP, Allen JD. Stable carbon isotopic composition of gasolines determined by isotope ratio monitoring gas chromatography mass spectrometry. Org Geochem. 2002;33(2):149–59.

Stiver W, Mackay D. Evaporation rate of spills of hydrocarbons and petroleum mixtures. Environ Sci Technol. 1984;18(11):834–40.

Ten Haven HL. Applications and limitations of Mango's light hydrocarbon parameters in petroleum correlation studies. Org Geochem. 1996;24(10–11):957–76.

Thompson KFM. Classification and thermal history of petroleum based on light hydrocarbons. Geochim Cosmochim Acta. 1983;47(2):303–16.

Thompson KFM. Fractionated aromatic petroleums and the generation of gas-condensates. Org Geochem. 1987;11(6):573–90.

Thompson KFM. Gas-condensate migration and oil fractionation in deltaic systems. Mar Pet Geol. 1988;5(3):237–46.

Wang Y, Huang YS. Hydrogen isotopic fractionation of low molecular weight *n*-alkanes during progressive vaporization. Org Geochem. 2001;32(8):991–8.

Wang Y, Huang YS. Hydrogen isotopic fractionation of petroleum hydrocarbons during vaporization: implications for assessing artificial and natural remediation of petroleum contamination. Appl Geochem. 2003;18(10):1641–51.

Wever HE. Petroleum and source rock characterization based on $C_7$ star plot results: examples from Egypt. Bull Am Assoc Pet Geol. 2000;84(7):1041–54.

Whiticar MJ, Snowdon LR. Geochemical characterization of selected Western Canada oils by $C_5$–$C_8$ compound specific isotope correlation (CSIC). Org Geochem. 1999;30(9):1127–61.

Xiao QL, Sun YG, Zhang YD, et al. Stable carbon isotope fractionation of individual light hydrocarbons in the $C_6$–$C_8$ range in crude oil as induced by natural evaporation: experimental results and geological implications. Org Geochem. 2012;50:44–56.

Zhang CM, Li ST, Zhao HJ, et al. Applications of Mango's light hydrocarbon parameters to petroleum from Tarim basin, NW China. Appl Geochem. 2005;20(3):545–51.

Zwank L, Berg M, Schmidt TC, et al. Compound-specific carbon isotope analysis of volatile organic compounds in the low-microgram per liter range. Anal Chem. 2003;75(20):5575–83.